IV．研究成果に関する刊行物

Neuromuscular

RESEARCH PAPER

Mutation profile of the *GNE* gene in Japanese patients with distal myopathy with rimmed vacuoles (GNE myopathy)

Anna Cho,[1] Yukiko K Hayashi,[1,2,3] Kazunari Monma,[1] Yasushi Oya,[4] Satoru Noguchi,[1] Ikuya Nonaka,[1] Ichizo Nishino[1,2]

ABSTRACT
Background GNE myopathy (also called distal myopathy with rimmed vacuoles or hereditary inclusion body myopathy) is an autosomal recessive myopathy characterised by skeletal muscle atrophy and weakness that preferentially involve the distal muscles. It is caused by mutations in the gene encoding a key enzyme in sialic acid biosynthesis, UDP-*N*-acetylglucosamine 2-epimerase/*N*-acetylmannosamine kinase (GNE).
Methods We analysed the *GNE* gene in 212 Japanese GNE myopathy patients. A retrospective medical record review was carried out to explore genotype–phenotype correlation.
Results Sixty-three different mutations including 25 novel mutations were identified: 50 missense mutations, 2 nonsense mutations, 1 insertion, 4 deletions, 5 intronic mutations and 1 single exon deletion. The most frequent mutation in the Japanese population is c.1714G>C (p. Val572Leu), which accounts for 48.3% of total alleles. Homozygosity for this mutation results in more severe phenotypes with earlier onset and faster progression of the disease. In contrast, the second most common mutation, c.527A>T (p.Asp176Val), seems to be a mild mutation as the onset of the disease is much later in the compound heterozygotes with this mutation and c.1714G>C than the patients homozygous for c.1714G>C. Although the allele frequency is 22.4%, there are only three homozygotes for c.527A>T, raising a possibility that a significant number of c.527A>T homozygotes may not develop an apparent disease.
Conclusions Here, we report the mutation profile of the *GNE* gene in 212 Japanese GNE myopathy patients, which is the largest single-ethnic cohort for this ultra-orphan disease. We confirmed the clinical difference between mutation groups. However, we should note that the statistical summary cannot predict clinical course of every patient.

INTRODUCTION
GNE myopathy, which is also known as distal myopathy with rimmed vacuoles,[1] quadriceps sparing myopathy[2] or hereditary inclusion body myopathy (hIBM),[3] is an autosomal recessive myopathy characterised by skeletal muscle atrophy and weakness that preferentially involve the distal muscles such as the tibialis anterior. It is a progressive disease, whereby the symptoms of muscle weakness start to affect the patient from the second or third decade of life, and most of the patients become wheelchair-bound between twenties and sixties.[4] The

characteristic histopathological features in muscle biopsy include muscle fibre atrophy with the presence of rimmed vacuoles and intracellular congophilic deposits.[4][5] GNE myopathy is caused by mutations in the gene encoding a key enzyme in sialic acid biosynthesis, UDP-*N*-acetylglucosamine 2-epimerase/*N*-acetylmannosamine kinase (GNE).[6–8] Genetically confirmed GNE myopathy was initially recognised in Iranian Jews and Japanese,[7][9] but later appeared to be widely distributed throughout the world. More than 100 mutations in the *GNE* gene have been described up to date.

During the last decade, there has been extensive experimental work to elucidate the pathogenesis and to develop therapeutic strategies of GNE myopathy.[6][10–12] Better knowledge on the basis of those research achievements have currently enabled us to enter the era of clinical trial for human patients. At this moment, the identification of new GNE myopathy patients with precise genetic diagnosis and the expansion of global spectrum of *GNE* mutations are timely and important. Here, we report the molecular profile of Japanese GNE myopathy patients with a brief discussion of genotype–phenotype correlations.

METHODS
Patients
Two hundred and twelve patients from 201 unrelated Japanese families were included in this study. There were 117 female and 95 male patients. All cases were genetically confirmed as GNE myopathy. A retrospective medical record review was carried out to explore genotype–phenotype correlation. Informed consent was obtained for the collection of clinical data and extraction of DNA to perform mutation analysis.

Genetic analysis
DNA was extracted from peripheral blood leukocytes or skeletal muscle tissue. We used the previously described sequencing method to describe mutations at cDNA level.[7] All exons and splice regions of the *GNE* gene were sequenced. NM_005476.5 was used as a reference sequence. We screened 100 alleles from normal Japanese individuals to determine the significance of novel variations.

Pathological analysis
To evaluate histopathological phenotype according to genotype, we analysed muscle biopsies from two

most common genotype groups in Japanese population. Each of the three age-matched and biopsy site-matched samples from c.1714G>C homozygous group and c.1714G>C/c.527A>T compound heterozygous group was compared. Muscle samples were taken from biceps brachii and frozen with isopentane cooled in liquid nitrogen. Serial frozen sections of 10 μm were stained using a set of histochemical methods including haematoxylin-eosin and modified Gomori trichrome.

Statistical analysis

Statistics were calculated using GraphPad Prism 5 software (GraphPad Software, La Jolla, California, USA). Between-group comparison for clinical data was performed using one-way analysis of variance with Dunnett's post-test. All values are expressed as means±SD. We performed two-sided tests with a $p<0.05$ level of significance.

RESULTS

Mutation profile

We identified homozygous or compound heterozygous GNE mutations in all 212 patients (see online supplement 1). In total, 63 different mutations were found including 50 missense mutations, 2 nonsense mutations, 1 insertion, 4 deletions, 5 intronic mutations and 1 single exon deletion (figure 1). Twenty-five novel mutations were identified including 17 missense mutations, 4 small deletions, 3 intronic mutations and 1 single exon deletion (figure 1, see online supplement).

Twenty-one mutations were found to be shared between two or more unrelated families. The three mutations occurring most frequently in the Japanese population were c.1714G>C (p.Val572Leu), c.527A>T (p.Asp176Val) and c.38G>C (p.Cys13Ser); these comprised 48.3%, 22.4% and 3.5%, respectively, of the total number of alleles examined (table 1).

Genotype–phenotype correlations

The mean age of genetic analysis was 41.6±14.1 years (n=212), and the mean age of symptom onset based on the data available was 28.4±10.2 years (n=195). The earliest onset age was 10 and the latest was 61 years old in our cohort. Thirty-six among 154 patients (23.4%) were full-time wheelchair users at the point of genetic diagnosis with the average age at loss of ambulation being 36.8±11.3 years (n=36). The youngest wheelchair-bound age was 19, and the oldest ambulant age was 78. To investigate genotype–phenotype correlations in the major GNE mutations of Japanese population, we compared the age at symptom onset and loss of ambulation between the patients groups carrying either of the two most frequent mutations, c.1714G>C and c.527A>T (table 2). As with a previous report,[13] homozygous c.1714G>C mutations resulted in earlier

Table 1 Allele frequency for GNE mutations in 212 Japanese GNE myopathy patients

Mutation type	Allele frequency
Missense	402 (94.8%)
Nonsense	3 (0.7%)
Insertion	1 (0.2%)
Small deletion	4 (0.9%)
Single exon deletion	2 (0.5%)
Intron	12 (2.8%)
Three most common mutations	
c.1765G>C (p.Val572Leu)	205 (48.3%)
c.578A>T (p.Asp176Val)	95 (22.4%)
c.38G>C (p.Cys13Ser)	15 (3.5%)
Total alleles	424

symptom onset (23.9±7.1 years, $p<0.01$) and the majority of full-time wheelchair users were in this group. On the other hand, c.1714G>C/c.527A>T compound heterozygous patients first developed symptoms at a later age (37.6±12.6 years, $p<0.01$), and there were no wheelchair-bound patients at the time of genetic analysis in this group. Only three homozygous c.527A>T mutation patients were identified, and their average onset age (32.3±5.7 years) was also higher among total patients (28.4±10.2 years). All three patients were ambulant until the last follow-up visits (29, 40 and 44 years).

Among 212 cases, 80 patients underwent muscle biopsies. Overall pathological findings in our series were compatible with GNE myopathy. The characteristic rimmed vacuoles were observed in the majority (76/80, 95.0%) of the cases. Through the analysis of muscle biopsies from age-matched and biopsy site-matched samples, we found that the histopathological phenotypes were in line with these genotype–phenotype correlations (figure 2). Homozygous c.1714G>C mutations have led to much more advanced pathological changes with severe myofibre atrophy and increased numbers of rimmed vacuoles. Marked adipose tissue replacement was appreciated in a case with reflecting very advanced stage of muscle degeneration.

DISCUSSION

As shown in figure 1, mutations were located throughout the whole open reading frame of the GNE gene. The majority (94.8%, 402/424 alleles) of the mutations in our series were missense mutations (table 1), and there were no homozygous null mutations. These results are in accordance with previous reports[7][9] signifying that total loss of GNE function might be
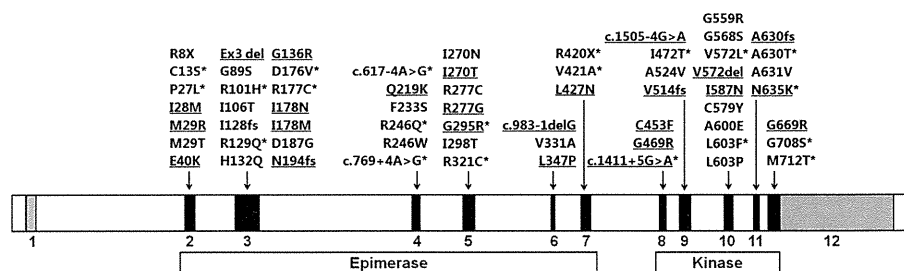

Figure 1 Mutation spectrum of GNE in the Japanese population. The mutations are located throughout the whole open reading frame. Twenty-five novel mutations are underlined, and 21 shared mutations are indicated with asterisks.

- 18 -

Table 2 Comparison of clinical course between two most frequent GNE mutations in Japanese population

Mutations	Age at exam (years)		Age at onset (years)		Age at WB (years)		Ambulant
c.1714G>C/c.1714G>C	38.6±13.4	(n=71)	23.9±7.1	(n=65)**	35.4±10.6	(n=28)	n=22
c.1714G>C/other	32.3±13.2	(n=25)	21.9±6.8	(n=22)*	37.0±8.6	(n=4)	n=16
c.1714G>C/c.527A>T	48.9±14.1	(n=38)	37.6±12.6	(n=35)**		(n=0)	n=29
c.527A>T/c.527A>T	37.7±7.7	(n=3)	32.3±5.7	(n=3)		(n=0)	n=3
c.527A>T/other	41.3±11.1	(n=51)	30.6±8.0	(n=46)		(n=2)	n=33
other/other	49.8±14.7	(n=24)	28.8±9.5	(n=24)		(n=2)	n=16
Total	41.6±14.1	(n=212)	28.4±10.2	(n=195)	36.8±11.3	(n=36)	n=118

Dunnett's multiple comparison test (control: total patients) *p<0.05, **p<0.01.
Other: a mutation other than c.1714G>C and c.527A>T; WB, wheelchair-bound.

lethal in human beings. The embryonic lethality of null mutation in GNE had also been proved in the mouse model.[14] Only three of total 212 patients carried a nonsense mutation; clinical data were available for two of them. Interestingly, one patient with compound heterozygous c.22C>T (p.Arg8X)/c.1714G>C (p.Val572Leu) mutations developed his first symptoms at the age of 15, while the other patient with c.1258C>T (p. Arg420X)/c.527A>T (p.Asp176Val) mutations developed her symptoms much later, at the age of 45. The similar difference was also observed in the phenotypes of patients with frame-shift mutations. A patient carrying c.383insT (p.I128fs) and c.1714G>C (p.Val572Leu) mutations developed his first symptom at the age of 13, whereas another two patients with c.1541-4del4 (p.Val514fs)/c.527A>T (p.Asp176Val) and

c.581delA (p.N194fs)/c.527A>T (p.Asp176Val) mutations had later symptom onset, at the age of 30 and 32 years, respectively. This clinical variation can be explained as it reflects alternative missense mutations, because the two patients with very early onset shared the same missense mutation c.1714G>C, while the patients with the milder phenotype shared c.527A>T.

Among five intronic mutations identified in our series, c.617 −4A>G and c.769 + 4A>G were previously reported as pathological mutations.[7] [15] Three novel variants were located at splice junction of exon 6 (c.983–1delG), exon 8 (c.1411 +5G>A) and exon 9 (c.1505–4G>A), raising the high possibility of relevant exons skipping. These variants were not detected in 200 alleles from normal Japanese individuals and also in the single nucleotide polymorphism (SNP) database.
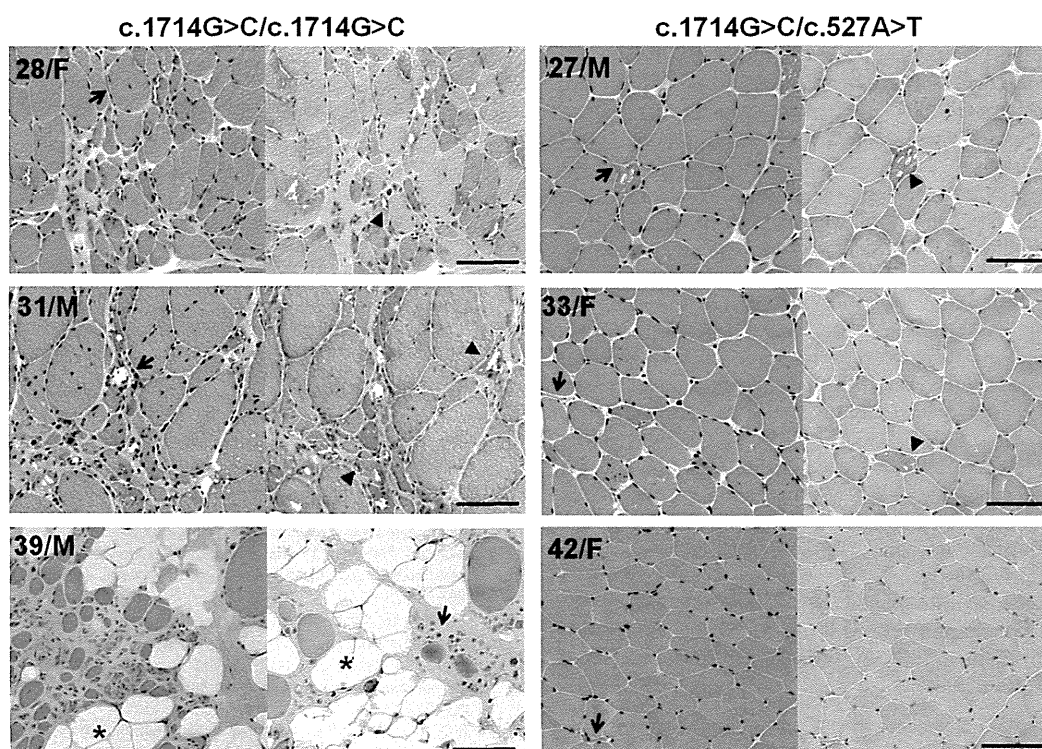
c.1714G>C/c.1714G>C

c.1714G>C/c.527A>T

Figure 2 Comparison of muscle pathology between patients with homozygous c.1714G>C (p.Val572Leu) and with compound heterozygous c.1714G>C (p.Val572Leu)/c.527A>T (p.Asp176Val) mutations. Homozygous c.1714G>C (p.Val572Leu) mutations have led to much more advanced histopathological changes compared with compound heterozygous c.1714G>C (p.Val572Leu)/c.527A>T (p.Asp176Val) mutations. Haematoxylin-eosin (left) and modified Gomori trichrome (right) stains of muscle sections from age (c.1714G>C/c.1714G>C: 28, 31 and 39 years, c.1714G>C/c.527A>T: 27, 33 and 42 years) and biopsy site (biceps brachii muscles) matched samples. Bar=100μm; triangles: rimmed vacuoles; arrows: atrophic fibres; asterisks: adipose tissue.

Neuromuscular

As there are ethnic differences in *GNE* mutation frequencies,[9] [16–19] establishing the mutation spectrum and defining predominant mutations in a certain population may be helpful for the diagnosis. Three most common mutations in the Japanese population and their allele frequencies (table 1) were in agreement with previous data.[7] [13] The allele frequencies of top two mutations (c.1714G>C and c.527A>T) comprise more than two-third of the total number of alleles suggesting that founder effects are involved in the relatively higher incidence of GNE myopathy in Japan.

Although most of patients showed characteristic pathological features, the existence of exceptional cases with atypical biopsy findings implies that GNE myopathy cannot be totally excluded from the absence of rimmed vacuoles in muscle biopsies. On the other hand, we found 94 patients who were pathologically or clinically suspected but not had mutations in *GNE*. Several cases of VCP myopathy mutations in (*VCP*), myofibrillar myopathy mutations in (*DES*) and reducing body myopathy (*FHL1*) were later identified in this group, suggesting these diseases should be included as differential diagnosis of GNE myopathy.[20]

In terms of genotype–phenotype correlations, we confirmed that homozygosity for c.1714G>C (p.Val572Leu) mutation resulted in more severe phenotypes in clinical and histopathological aspects. In contrast, the second most common mutation, c.527A>T (p.Asp176Val), seems to be a mild mutation as the onset of the disease is much later in the compound heterozygotes with this mutation and c.1714G>C. Several evidences further strengthened the link between the more severe phenotype and c.1714G>C, and between the milder phenotype and c.527A>T. Compound heterozygosity for c.1714G>C and non-c.527A>T mutations resulted in earlier symptom onset (22.9 ± 6.8 years, $p<0.05$) compared with the average onset age of the total group, whereas c.527A>T, both presented as homozygous and as compound heterozygous mutations, lead to slower disease progression (table 2). In addition, only three patients carrying this second most common mutation c.527A>T in homozygous mode were identified, which is much fewer than the number expected from high allele frequency (22.4%), raising a possibility that considerable number of c.527A>T homozygotes may not even develop a disease. In fact, we ever identified an asymptomatic c.527A>T homozygote at age 60 years.[7] Now he is at age 71 years and still healthy. Overall, these results indicate that different mutations lead to different spectra of severity. However, this is a result of a statistical summary that cannot predict clinical course of each individual patient.

Here, we presented the molecular bases of 212 Japanese GNE myopathy patients with 25 novel *GNE* mutations. Based on the current status of knowledge, sialic acid supplementation may lead to considerable changes in the natural course of GNE myopathy within near future. The ongoing identification of *GNE* mutations and further studies regarding the clinicopathological features of each mutation will provide better understanding of GNE myopathy and lead to accelerated development of treatment for this disease.

REFERENCES

1 Nonaka I, Sunohara N, Ishiura S, et al. Familial distal myopathy with rimmed vacuole and lamellar (myeloid) body formation. *J Neurol Sci* 1981;51:141–55.
2 Argov Z, Yarom R. "Rimmed vacuole myopathy" sparing the quadriceps. A unique disorder in Iranian Jews. *J Neurol Sci* 1984;64:33–43.
3 Askanas V, Engel WK. New advances in the understanding of sporadic inclusion-body myositis and hereditary inclusion-body myopathies. *Curr Opin Rheumatol* 1995;7:486–96.
4 Nonaka I, Noguchi S, Nishino I. Distal myopathy with rimmed vacuoles and hereditary inclusion body myopathy. *Curr Neurol Neurosci Rep* 2005;5:61–5.
5 Nishino I, Malicdan MC, Murayama K, et al. Molecular pathomechanism of distal myopathy with rimmed vacuoles. *Acta Myol* 2005;24:80–3.
6 Eisenberg I, Avidan N, Potikha T, et al. The UDP-N-acetylglucosamine 2-epimerase/N-acetylmannosamine kinase gene is mutated in recessive hereditary inclusion body myopathy. *Nat Genet* 2001;29:83–7.
7 Nishino I, Noguchi S, Murayama K, et al. Distal myopathy with rimmed vacuoles is allelic to hereditary inclusion body myopathy. *Neurology* 2002;59:1689–93.
8 Keppler OT, Hinderlich S, Langner J, et al. UDP-GlcNAc 2-epimerase: a regulator of cell surface sialylation. *Science* 1999;284:1372–6.
9 Eisenberg I, Grabov-Nardini G, Hochner H, et al. Mutations spectrum of *GNE* in hereditary inclusion body myopathy sparing the quadriceps. *Hum Mutat* 2003;21:99.
10 Noguchi S, Keira Y, Murayama K, et al. Reduction of UDP-N-acetylglucosamine 2-epimerase/N-acetylmannosamine kinase activity and sialylation in distal myopathy with rimmed vacuoles. *J Biol Chem* 2004;279:11402–7.
11 Malicdan MC, Noguchi S, Nonaka I, et al. A Gne knockout mouse expressing human *GNE* D176V mutation develops features similar to distal myopathy with rimmed vacuoles or hereditary inclusion body myopathy. *Hum Mol Genet* 2007;16:2669–82.
12 Malicdan MC, Noguchi S, Hayashi YK, et al. Prophylactic treatment with sialic acid metabolites precludes the development of the myopathic phenotype in the DMRV-hIBM mouse model. *Nat Med* 2009;15:690–5.
13 Mori-Yoshimura M, Monma K, Suzuki N, et al. Heterozygous UDP-GlcNAc 2-epimerase and N-acetylmannosamine kinase domain mutations in the *GNE* gene result in a less severe GNE myopathy phenotype compared to homozygous N-acetylmannosamine kinase domain mutations. *J Neurol Sci* 2012;318:100–5.
14 Schwarzkopf M, Knobeloch KP, Rohde E, et al. Sialylation is essential for early development in mice. *Proc Natl Acad Sci USA* 2002;99:5267–70.
15 Ikeda-Sakai Y, Manabe Y, Fujii D, et al. Novel Mutations of the *GNE* gene in distal myopathy with rimmed vacuoles presenting with very slow progression. *Case Rep Neurol* 2012;4:120–5.
16 Li H, Chen Q, Liu F, et al. Clinical and molecular genetic analysis in Chinese patients with distal myopathy with rimmed vacuoles. *J Hum Genet* 2011;56:335–8.
17 Liewluck T, Pho-Iam T, Limwongse C, et al. Mutation analysis of the *GNE* gene in distal myopathy with rimmed vacuoles (DMRV) patients in Thailand. *Muscle Nerve* 2006;34:775–8.
18 Kim BJ, Ki CS, Kim JW, et al. Mutation analysis of the *GNE* gene in Korean patients with distal myopathy with rimmed vacuoles. *J Hum Genet* 2006;51:137–40.
19 Broccolini A, Ricci E, Cassandrini D, et al. Novel *GNE* mutations in Italian families with autosomal recessive hereditary inclusion-body myopathy. *Hum Mutat* 2004;23:632.
20 Shi Z, Hayashi YK, Mitsuhashi S, et al. Characterization of the Asian myopathy patients with VCP mutations. *Eur J Neurol* 2012;19:501–9.

– 20 –

Mutation profile of the *GNE* gene in Japanese patients with distal myopathy with rimmed vacuoles (GNE myopathy)

Anna Cho, Yukiko K Hayashi, Kazunari Monma, et al.

Updated information and services can be found at:
http://jnnp.bmj.com/content/early/2013/09/11/jnnp-2013-305587.1.full.html

These include:

Data Supplement	*"Supplementary Data"* http://jnnp.bmj.com/content/suppl/2013/09/11/jnnp-2013-305587.DC1.html
References	This article cites 20 articles, 4 of which can be accessed free at: http://jnnp.bmj.com/content/early/2013/09/11/jnnp-2013-305587.1.full.html#ref-list-1
P<P	Published online September 11, 2013 in advance of the print journal.
Email alerting service	Receive free email alerts when new articles cite this article. Sign up in the box at the top right corner of the online article.

Topic Collections	Articles on similar topics can be found in the following collections Muscle disease (200 articles) Musculoskeletal syndromes (432 articles) Neuromuscular disease (1064 articles)

Advance online articles have been peer reviewed, accepted for publication, edited and typeset, but have not not yet appeared in the paper journal. Advance online articles are citable and establish publication priority; they are indexed by PubMed from initial publication. Citations to Advance online articles must include the digital object identifier (DOIs) and date of initial publication.

To request permissions go to:
http://group.bmj.com/group/rights-licensing/permissions

To order reprints go to:
http://journals.bmj.com/cgi/reprintform

To subscribe to BMJ go to:
http://group.bmj.com/subscribe/

– 22 –

Notes

Advance online articles have been peer reviewed, accepted for publication, edited and typeset, but have not not yet appeared in the paper journal. Advance online articles are citable and establish publication priority; they are indexed by PubMed from initial publication. Citations to Advance online articles must include the digital object identifier (DOIs) and date of initial publication.

To request permissions go to:
http://group.bmj.com/group/rights-licensing/permissions

To order reprints go to:
http://journals.bmj.com/cgi/reprintform

To subscribe to BMJ go to:
http://group.bmj.com/subscribe/

GNE myopathy in India

Atchayaram Nalini, Narayanappa Gayathri[1], Ischizo Nishino[2,3], Yukiko K. Hayashi[2,3]

Departments of Neurology and [1]Neuropathology, National Institute of Mental Health and Neurosciences, Bangalore, Karnataka, India, [2]Department of Neuromuscular Research, National Institute of Neuroscience, Tokyo [3]Department of Clinical Development, Translational Medical Center, National Center of Neurology and Psychiatry, Tokyo, Japan

Address for correspondence:
Dr. Atchayaram Nalini,
Department of Neurology,
National Institute of Mental
Health and Neurosciences,
Bangalore - 560 029, Karnataka, India.
E-mail: atchayaramnalini@yahoo.co.in

Abstract

Background: *GNE* myopathy is a clinicopathologically distinct distal myopathy with autosomal-recessive inheritance. The *GNE* gene mutations are known to cause this form of distal myopathy **Materials and Methods:** Over the last 6 years, a total of 54 patients from 48 families were diagnosed to have *GNE* myopathy based on the clinical and histopathological findings. We have reported on 23 cases earlier and from this cohort 12 patients from 11 families underwent genetic testing for *GNE* mutation. **Results:** Nine patients belonging to eight families were confirmed as *GNE* myopathy by genetic analysis. There were six women and three men. Mean age of onset was 26.7 ± 5.47 years (20-36 years) and mean age at clinical examination was 32.3 ± 4.2 years (28-39 years). Mean duration of the illness was 5.7 ± 4.7 years (1-14 years). All had characteristic clinical features of progressive weakness and wasting of the anterior part of leg muscles, adductors of thighs and hamstrings with relative sparing of the quadriceps muscles. Biopsy from the tibialis anterior muscles revealed the presence of rimmed vacuoles. Mutation analysis of the *GNE* gene revealed that c. 2086G > A (p.Val696Met) change was common in our series like Thailand and six of eight families carried this mutation, heterozygously. **Conclusion:** These results show the presence of a common mutation in *GNE* gene in Southeast Asia.

Key words: c. 2086G > A (p.Val696Met), GNE myopathy, mutation analysis

Introduction

GNE myopathy also called as distal myopathy with rimmed vacuoles (DMRV), hereditary inclusion body myopathy (hIBM), quadriceps-sparing myopathy or Nonaka myopathy is a clinicopathologically distinct distal myopathy with autosomal-recessive inheritance. It is clinically characterized by preferential involvement of anterior tibial muscles and sparing of quadriceps and pathologically by the presence of rimmed vacuoles (RV) on muscle biopsy.[1-3] The age of onset ranges from 15 to 40 years.[4] Patients generally become wheelchair bound between 26 and 57 years of age, on an average

12 years after the onset of symptoms.[4] Serum creatine kinase (CK) level is normal or mildly elevated.

The *GNE* gene mutations are known to cause this form of distal myopathy.[5,6] *GNE* encodes a bifunctional enzyme, uridine diphosphate-N-acetylglucosamine 2-epimerase/ N-acetylmannosamine kinase, which plays a critical role in the production of sialic acid.[7] *GNE* mutations are reported to be responsible for a lower level of sialic acid in skeletal muscles, which is postulated to be causative of the diseases.[8] Recently, limb girdle phenotype is reported to be frequent presentation in patients with myopathy associated with *GNE* mutations.[9] In the present report, we describe 9 patients with *GNE* myopathy who underwent *GNE* mutation studies.

Materials and Methods

Institutional ethical approval was obtained for the study. Muscle biopsies are routinely performed for diagnostic purpose. Written informed consent was obtained from all patients who approached for genetic analysis. Nine adult

Access this article online	
Quick Response Code:	**Website:** www.neurologyindia.com
	PMID: ***
	DOI: 10.4103/0028-3886.117609

patients who belonged to the original cohort of 23 cases were included in the present study.[10] All these patients were recruited from the Neuromuscular Disorders clinic at National Institute of Mental Health and Neurosciences, Bangalore, India. All patients attending the clinic undergo a thorough phenotypic characterization. An exhaustive proforma is completed for the topography of muscle involvement. *GNE* myopathy was diagnosed based on the following proposed findings (i) autosomal-recessive inheritance, but may be sporadic, (ii) onset of symptoms in early adulthood (iii) weakness beginning in the distal leg muscles, typically in the anterior tibialis muscles, with the quadriceps muscles remaining relatively unaffected, (iv) myogenic changes on electromyography, (v) normal or mildly elevated serum CK, (vi) muscle biopsies displaying RV without obvious dystrophic features.[1,11,12]

Genetic analysis

Genomic DNA was extracted from peripheral blood lymphocytes using the standard techniques. All exons and their flanking intronic regions of *GNE* were sequenced directly using an ABI PRISM 3130 automated sequencer (PE Applied Biosystems). The primer sequences used in this study are available on request. We used the GenBank NM_001190383 for the description of the mutations.

Results

Clinical features

We examined nine patients (six women and three men) who had weakness and atrophy of peroneal muscles with relatively preserved to normal power in quadriceps muscles. Onset of the disease was in the second or third decade in the majority and the mean age of onset was 26.7 ± 5.4 (20-36) years. Mean age at clinical examination was 32.3 ± 4.2 years (28-39). Mean duration of illness was 5.6 ± 4.7 (1-14) years. Details of the clinical manifestations, investigations and mutation findings are represented in Table 1. The initial symptom in the majority of the patients was altered gait. Muscle weakness was particularly prominent in tibialis anterior, hip adductors and hamstrings in the lower limbs with foot drop. Neck flexors were weak in majority. In upper limbs, distal and shoulder girdle muscles were more affected than arm muscles. The long finger flexors were particularly weak. Within months to a few years, the patients developed muscle weakness of the proximal lower and the distal upper limbs. All patients had minimal or no involvement in quadriceps muscles and was ambulant at the time of evaluation except for three severely disabled patients (case three, four, five and seven). Serum CK levels were normal to only slightly elevated.

Mutation analysis of *GNE*

We identified mutations in *GNE* in all 8 families examined. One consanguineous family (F1) had a homozygousc. 484C > T (p.Arg162Cys) mutation, which is previously reported.[13] Four had a compound heterozygous mutations including two novel missense mutations of c. 910G > A (p.Gly304Arg) and c. 1703G > T (p.Gly568Val) and two previously reported nonsense mutations of c. 1258C > T (p.Arg420X) andc. 1539G > A (p.Trp513X).[14] A c. 2086G > A (p.Val696Met) mutation was commonly seen in our series and identified in the six of eight families (75%), heterozygously. Four patients in three families (F6-8) had only one heterozygous reported mutation.

Discussion

Familial vacuolar myopathy with autosomal-recessive inheritance characterized clinically by progressive distal and proximal muscle wasting and weakness beginning in early adulthood and almost always sparing the quadriceps femoris even in advanced stages was reported to occur in Jews of Persian origin.[15,16] The familial myopathy in Persian Jews has been considered to be an autosomal-recessive form of hIBM, which is now called as *GNE* myopathy.[17-19] Our patients all had the classical clinical and histopathological features of *GNE* myopathy.

Over the last 6 years, we have diagnosed 54 patients phenotypically having the classical features of *GNE* myopathy and muscle biopsy confirming the diagnosis of rimmed vacuolar myopathy. Our earlier report on 23 cases was based on the clinical and histopathological features.[10] The initial and preferential peroneal muscle involvement appears in the second or third decade of life in most patients and the disease is progressive, usually leading to a non-ambulant state within 10 years after the onset.[1-3]

Nonaka *et al.*, for the first time described three patients from two families of Japanese origin with autosomal-recessive inheritance and presence of RV in muscle biopsies.[11] DMRV or now termed as *GNE* myopathy is a distinct clinical entity inherited through an autosomal-recessive trait with female preponderance.[3] The mean age of onset in our group was 26.7 years and the initial symptoms of muscle weakness of the legs appeared in the majority in the second or third decade. In a review of 37 Japanese patients, the mean age of onset was 26.1 and onset in the third decade was noted in 64% of the patients.[20] Clinically in seven of their nine patients in whom duration of illness was more than 10 years, five of them became non-ambulatory. Serum CK was mildly

– 24 –

Table 1: Clinical characteristics and investigation findings in the nine cases with GNE mutation analyses

Parameters	Case 1	Case 2	Case 3	Case 4	Case 5	Case 6	Case 7 (Sibling of case 6)	Case 8	Case 9
Gender	M	F	F	F	M	F	F	M	F
Age at onset (year)	26	26	34	20	25	20	26	27	36
Duration of illness (year)	8	2	1	10	14	9	3	2	2
Symptom at onset	Foot drop	Foot drop	Foot drop	Foot drop	Foot drop	Foot drop	Foot drop	Foot drop	Foot drop
Symm/Asymat onset	Asym	Asym	Symm	Asym	Symm	Asym	Symm	Symm	Asym
Consanguinity	Yes	No	No	No	No	Yes	Yes	Yes	No
Family history	No	No	No	No	No	Yes	Yes	No	Yes
Serum CK (IU)	238	520	496	116	496	132	445	230	189
MRC power (grade)									
Shoulder	5	5	5	1	4	1	4	3	5
Elbow	5	5	5	1	4	2	4	3	5
Long flexors of hand	4	3	4	2	2	1	2	2	2
Small muscle of hand	4	4	4	1	2	1	2	2	2
Iliopsoas	4	1	2	0	2	1	1	2	1
Glut Max	4	4	4	0	3	1	2	3	3
Adductors	3	1	1	0	2	1	0	3	1
Abductors	4	4	5	0	3	1	3	3	3
Quadriceps	4	5	5	2	5	1	5	3	5
Hamstrings	3	2	2	0	2	1	1	2	2
Ankle									
Dorsiflexors	1	1	3	1	0	1	0	2	2
Plantarflexors	4	3	5	1	2	1	3	4	5
At evaluation	Ambulant	Ambulant	Ambulant	WCB	Ambulant with support	WCB	WCB	Ambulant	Assistance
Muscle biopsy (RV's)	Present	Present	Present	Present	Present	Present	Present	Present	Present
Mutation									
Nucleotide substitution	c.484C>T (homo)	c.910G>A/c. 2086G>A	c.1258C>T/c. 2086G>A	c.1539G>A/c. 2086G>A	c.1703G>T/c. 2086G>A	c.2086G>A/?	c.2086G >A/?	c.2086G >A/?	c.80C>T/?
Exon domain	Epimerase/ epimease	Epimerase/ kinase	Kinase/ kinase	Kinase/ kinase	Kinase/ kinase	Kinase/?	Kinase/?	Kinase/?	Epimerase/?
Amino acid substitution	Arg162Cys (homo)	Gly304Arg/ Val696Met	Arg420X/ Val696Met	Trp513X/ Val696Met	Gly568Val/ Val696Met	Val696Met/?	Val696Met/?	Val696Met/?	Pro27 Leu/?

Y - Years, Symm - Symmetrical, Asym - Asymmetrical, CK - Creatine kinase, Glut - Gluteus, Max - Maximus, RV - Rimmed vacuoles, WCB - Wheel chair bound, MRC - Medical research council

elevated or within the normal limits among the 37 Japanese patients. CK levels in our cohort were normal or minimally elevated.

In the present study, genetic analysis identified a homozygous c. 484C > T (p.Arg162Cys) mutation in one family. This mutation was previously reported in an Italian family.[13] Four families had a compound heterozygous mutations including 2 novel missense mutations c. 910G > A (p.Gly304Arg) and c. 1703G > T (p.Gly568Val). Both these amino acids are well-preserved among species and a missense mutation p.Gly568Ser was also recently identified in a Japanese GNE myopathy patient.[21] The c. 2086G > A (p.Val696Met) mutation was common in this series and identified in the six of eight families (75%), heterozygously. This mutation was reported previously among patients from Thailand.[7,21]

In GNE myopathy, presence of the common mutation is known to occur in different ethnic backgrounds, i.e. p. Val572 Leu mutation in Japanese and Korean patients and p.Met712Thr in the Jewish population. Findings in the present study and earlier studies, p.Val696Met substitution appears to be the most common mutation in both India and Thailand.[22] In this study, four patients from three families had only one heterozygous mutation in GNE gene. The second mutation may not be detectable using the present method, which detects only large deletions in the GNE gene. In a previous study from Japan, patients with a nonsense mutation in one allele showed relatively severe clinical features.[21] However, in this series, one patient (case 3) of 34 years of age harboring p.Arg420X/Val696Met mutation was ambulant, but had illness onset at 33 years of age while case 4 (30 years of age) with p.Try513X/Val696Met was wheel chair-bound after 10 years of illness duration.

- 25 -

From the predicted structure models reported by Kurochkina, *et al.*, p.Arg420X can preserve its epimerase activity and the enzyme hexameric state, whereas p.Try513X causes its conformational change on glucose binding if these proteins are produced.[23] This study confirms that *GNE* myopathy may be indeed one among the common inherited myopathies among Indians. Further analysis in a larger cohort is required to clarify the genotype-phenotype correlations of *GNE* myopathy among Indian population.

References

1. Nonaka I, Sunohara N, Satoyoshi E, Terasawa K, Yonemoto K. Autosomal recessive distal muscular dystrophy: A comparative study with distal myopathy with rimmed vacuole formation. Ann Neurol 1985;17:51-9.
2. Argov Z, Yarom R. Rimmed vacuole myopathy sparing the quadriceps. A unique disorder in Iranian Jews. J Neurol Sci 1984;64:33-43.
3. Nishino I, Noguchi S, Murayama K, Driss A, Sugie K, Oya Y, et al. Distal myopathy with rimmed vacuoles is allelic to hereditary inclusion body myopathy. Neurology 2002;59:1689-93.
4. Nonaka I, Noguchi S, Nishino I. Distal myopathy with rimmed vacuoles and hereditary inclusion body myopathy. Curr Neurol Neurosci Rep 2005;5:61-5.
5. Arai A, Tanaka K, Ikeuchi T, Igarashi S, Kobayashi H, Asaka T, et al. A novel mutation in the GNE gene and a linkage disequilibrium in Japanese pedigrees. Ann Neurol 2002;52:516-9.
6. Argov Z, Tiram E, Eisenberg I, Sadeh M, Seidman CE, Seidman JG, et al. Various types of hereditary inclusion body myopathies map to chromosome 9p1-q1. Ann Neurol 1997;41:548-51.
7. Eisenberg I, Avidan N, Potikha T, Hochner H, Chen M, Olender T, et al. The UDP-N-acetylglucosamine 2-epimerase/N-acetylmannosamine kinase gene is mutated in recessive hereditary inclusion body myopathy. Nat Genet 2001;29:83-7.
8. Noguchi S, Keira Y, Murayama K, Ogawa M, Fujita M, Kawahara G, et al. Reduction of UDP-N-acetylglucosamine 2-epimerase/N-acetylmannosamine kinase activity and sialylation in distal myopathy with rimmed vacuoles. J Biol Chem 2004;279:11402-7.
9. Park YE, Kim HS, Choi ES, Shin JH, Kim SY, Son EH, et al. Limb-girdle phenotype is frequent in patients with myopathy associated with GNE mutations. J Neurol Sci 2012;321:77-81.
10. Nalini A, Gayathri N, Dawn R. Distal myopathy with rimmed vacuoles: Report on clinical characteristics in 23 cases. Neurol India 2010;58:235-41.
11. Nonaka I, Sunohara N, Ishiura S, Satoyoshi E. Familial distal myopathy with rimmed vacuole and lamellar (myeloid) body formation. J Neurol Sci 1981;51:141-55.
12. Mizusawa H, Kurisaki H, Takatsu M, Inoue K, Mannen T, Toyokura Y, et al. Rimmed vacuolar distal myopathy: A clinical, electrophysiological, histopathological and computed tomographic study of seven cases. J Neurol 1987;234:129-36.
13. Del Bo R, Baron P, Prelle A, Serafini M, Moggio M, Fonzo AD, et al. Novel missense mutation and large deletion of GNE gene in autosomal-recessive inclusion-body myopathy. Muscle Nerve 2003;28:113-7.
14. Tomimitsu H, Ishikawa K, Shimizu J, Ohkoshi N, Kanazawa I, Mizusawa H. Distal myopathy with rimmed vacuoles: Novel mutations in the GNE gene. Neurology 2002;59:451-4.
15. Ro LS, Lee-Chen GJ, Wu YR, Lee M, Hsu PY, Chen CM. Phenotypic variability in a Chinese family with rimmed vacuolar distal myopathy. J Neurol Neurosurg Psychiatry 2005;76:752-5.
16. Sadeh M, Gadoth N, Hadar H, Ben-David E. Vacuolar myopathy sparing the quadriceps. Brain 1993;116:217-32.
17. Askanas V, Engel WK. New advances in inclusion-body myositis. Curr Opin Rheumatol 1993;5:732-41.
18. Askanas V, Engel WK. New advances in the understanding of sporadic inclusion-body myositis and hereditary inclusion-body myopathies. Curr Opin Rheumatol 1995;7:486-96.
19. Griggs RC, Askanas V, DiMauro S, Engel A, Karpati G, Mendell JR, et al. Inclusion body myositis and myopathies. Ann Neurol 1995;38:705-13.
20. Sunohara N, Nonaka I, Kamei N, Satoyoshi E. Distal myopathy with rimmed vacuole formation. A follow-up study. Brain 1989;112:65-83.
21. Mori-Yoshimura M, Monma K, Suzuki N, Aoki M, Kumamoto T, Tanaka K, et al. Heterozygous UDP-GlcNAc 2-epimerase and N-acetylmannosamine kinase domain mutations in the GNE gene result in a less severe GNE myopathy phenotype compared to homozygous N-acetylmannosamine kinase domain mutations. J Neurol Sci 2012;318:100-5.
22. Liewluck T, Pho-Iam T, Limwongse C, Thongnoppakhun W, Boonyapisit K, Raksadawan N, et al. Mutation analysis of the GNE gene in distal myopathy with rimmed vacuoles (DMRV) patients in Thailand. Muscle Nerve 2006;34:775-8.
23. Kurochkina N, Yardeni T, Huizing M. Molecular modeling of the bifunctional enzyme UDP-GlcNAc 2-epimerase/ManNAc kinase and predictions of structural effects of mutations associated with HIBM and sialuria. Glycobiology 2010;20:322-37.

EMBO
Molecular Medicine

OPEN ACCESS　TRANSPARENT PROCESS

Defects of Vps15 in skeletal muscles lead to autophagic vacuolar myopathy and lysosomal disease

Ivan Nemazanyy[1,2], Bert Blaauw[3], Cecilia Paolini[4], Catherine Caillaud[1,2], Feliciano Protasi[4], Amelie Mueller[5], Tassula Proikas-Cezanne[5], Ryan C. Russell[6], Kun-Liang Guan[6], Ichizo Nishino[7], Marco Sandri[3], Mario Pende[1,2]*, Ganna Panasyuk[1,2]

The complex of Vacuolar Protein Sorting 34 and 15 (Vps34 and Vps15) has Class III phosphatidylinositol 3-kinase activity and putative roles in nutrient sensing, mammalian Target Of Rapamycin (mTOR) activation by amino acids, cell growth, vesicular trafficking and autophagy. Contrary to expectations, here we show that *Vps15*-deficient mouse tissues are competent for LC3-positive autophagosome formation and maintain mTOR activation. However, an impaired lysosomal function in mutant cells is traced by accumulation of adaptor protein p62, LC3 and Lamp2 positive vesicles, which can be reverted to normal levels after ectopic overexpression of Vps15. Mice lacking Vps15 in skeletal muscles, develop a severe myopathy. Distinct from the autophagy deficient *Atg7*^{−/−} mutants, pathognomonic morphological hallmarks of autophagic vacuolar myopathy (AVM) are observed in *Vps15*^{−/−} mutants, including elevated creatine kinase plasma levels, accumulation of autophagosomes, glycogen and sarcolemmal features within the fibres. Importantly, Vps34/Vps15 overexpression in myoblasts of Danon AVM disease patients alleviates the glycogen accumulation. Thus, the activity of the Vps34/Vps15 complex is critical in disease conditions such as AVMs, and possibly a variety of other lysosomal storage diseases.

INTRODUCTION

The *vps34* and *vps15* genes were initially identified in yeast screens for mutants defective in protein localization, sorting and processing to the vacuole, the equivalent of mammalian lysosome (Banta et al, 1988; Robinson et al, 1988). *vps34* and

(1) Inserm, U845, Paris, France
(2) Université Paris Descartes, Faculté de Médecine, UMRS-845, Paris, France
(3) Venetian Institute of Molecular Medicine, Padova, Italy
(4) Dipartimento Neuroscienze Imaging, Università "G. d'Annunzio", Chieti, France
(5) Eberhard Karls University Tuebingen, Tuebingen, Germany
(6) Department of Pharmacology and Moores Cancer Center, University of California, San Diego, La Jolla, CA, USA
(7) National Institute of Neuroscience, National Center of Neurology and Psychiatry, Tokyo, Japan
*Corresponding author: Tel: +33 1 72 60 63 86; Fax: +33 1 72 60 64 01;
E-mail: mario.pende@inserm.fr

vps15 mutant yeast strains display severe defects in the sorting and delivery of soluble hydrolases, including carboxypeptidase Y, from the late Golgi to the vacuole. Another striking phenotype of these mutants is impaired macroautophagy (hereafter referred to as autophagy), a major process in response to starvation conditions (Kihara et al, 2001). Autophagy begins with the formation of an autophagosome, a double membrane structure that engulfs parts of the cytoplasm and whole organelles, and ultimately fuses with a lysosome to enable degradation of the enclosed material (Mehrpour et al, 2010). Vps34 and Vps15 proteins are obligate partners acting in a complex. Vps34 is a Class III phosphatidylinositol 3-kinase (PI3K) converting phosphatidylinositol (PI) to phosphatidyl-inositol 3-phosphate (PI3P) (Schu et al, 1993), while Vps15 is a regulatory subunit with putative serine/threonine kinase activity and is required for Vps34 stability and activation (Schu et al, 1993). The conservation of *Vps15* and *Vps34* genes from yeast to mammals suggests their evolutionary conserved role in

essential cellular functions, prompting the phenotypic analysis of mammalian mutants.

The different functions of Vps34/Vps15 appear to be mediated by specific complexes. Atg6 and Vps38 are additional partners of Vps34/Vps15 in a protein complex for carboxy-peptidase Y sorting, while a complex containing Vps34, Vps15, Atg6 and Atg14, but not Vps38, is required in yeast for autophagy (Kihara et al, 2001). In mammals at least three different Vps15/Vps34 complexes regulate different stages of autophagy. Each complex contains Beclin 1, the mammalian orthologue of Atg6. An Atg14-like (Atg14L) containing complex stimulates autophagosome formation, while ultraviolet radia-tion resistance-associated gene protein (UVRAG, the putative orthologue of Vps38) belongs to a complex that enhances or suppresses the maturation of autophagosome and endosome depending on the presence of the Rubicon protein (Matsunaga et al, 2009; Zhong et al, 2009). The existence of additional functions carried by distinct complexes has been postulated, as RNAi against Vps34 and Vps15 down-regulates mammalian Target Of Rapamycin (mTOR, now officially named mechanistic Target Of Rapamycin) activity upon amino acid stimulation in human cells (Byfield et al, 2005; Nobukuni et al, 2005; Yoon et al, 2011). Since mTOR is a known negative regulator of autophagy (Jung et al, 2010), these findings would therefore imply that different Vps15/Vps34 complexes might be somehow activated in opposite environmental conditions. Beclin 1 containing complexes may regulate autophagy during starva-tion while Beclin 1-independent complexes may up-regulate mTOR during amino acid stimulation. Thus, Vps34/Vps15 can mediate sequential, complementary or opposite responses to nutrient availability depending on the partners and environ-mental conditions. Clearly, the physiological outcomes of varying Vps34/Vps15 activity are difficult to predict.

Muscle tissue is one of the most adaptable tissues in the body as it needs to respond promptly to different physiological conditions, such as exercise, loading and diet modification. For these reasons skeletal muscle requires a rapid and efficient system for removal of altered organelles, elimination of protein aggregates and disposal of toxic products, which can block proper contraction of sarcomeres. Not surprisingly muscle tissue is one of the most responsive tissue to autophagy activation (Mizushima et al, 2004). Consistently, alterations of autophagosome and lysosome functions have important con-sequences on skeletal muscle pathophysiology (Sandri, 2010). Both, an excess and a reduced levels of autophagy are detrimental for muscle function. Deficiency in mouse skeletal muscles of *Atg7*, an autophagy gene encoding the E1-like enzyme of ubiquitin-like conjugation systems essential for the autophagosome biogenesis, leads to a 20% reduction of muscle mass and specific force with signs of degeneration that are especially evident in muscle wasting conditions (Masiero et al, 2009). Human myopathies due to lack of collagen VI, such as Ullrich dystrophies and Bethlem myopathies, display defective basal autophagy and symptoms are ameliorated by inducing autophagy with diet or pharmacological interventions (Grumati et al, 2010). Conversely, the accumulation of autophagosomes is a pathognomonic feature in other classes of myopathies

including autophagic vacuolar myopathies (AVMs), lysosomal storage diseases, inclusion body myopathy with rimmed vacuoles Paget disease of bone-frontotemporal dementia (IBMPFD) (Nishino, 2003). Interestingly, loss of function mutations in myotubularins, the lipid phosphatases that specifically dephosphorylate PI3P and PI(3,5)P$_2$ at the D3 position, have been associated with myopathies and defects in the inhibition of autophagy. In particular, myotubularin 1 (*MTM1*) mutations lead to X-linked myotubular myopathy (Beggs et al, 2010), and Jumpy (*MTMR14*) mutations cause congenital disease centronuclear myopathy (Vergne and Deretic, 2010). However, the involvement of Vps34/Vps15 complexes in these muscle diseases has not been addressed.

Here we investigate the effects of Vps15/Vps34 inactivation in the mouse whole body, in mouse embryonic fibroblasts (MEFs), myotubes and in skeletal muscles after genetic deletion of the *Vps15* gene (also known as *Phosphoinositide-3-Kinase, regulatory subunit 4—PIK3R4*). We show that the deletion of the N-terminus region of Vps15 containing putative catalytic domain is sufficient to affect Vps34 expression and activity. Surprisingly, mutant cells do not show impaired mTOR activation by nutrients, despite a severe effect on viability. The capacity of autolysosome clearance is profoundly impaired in *Vps15*-deficient MEFs, myotubes and muscles *in vivo*, while the induction of autophagy is not blocked. Moreover, *Vps15$^{-/-}$* muscles suffer of AVM characterized by profound muscle weakness and massive accumulation of autophagosomal and lysosomal structures. Finally, human cells from AVM patients display reduced signs of lysosomal storage disease upon ectopic overexpression of Vps15 and Vps34 complex.

RESULTS

Generation of *Vps15*-null mice and cells

To study the function of Vps15 *in vivo* we introduced by homologous recombination two loxP sites flanking exon 2 of the *Vps15* gene. Exon 2 contains the start ATG codon, and encodes the myristoylation signal sequence for membrane localization and putative protein kinase domain including ATP-binding site (Fig. 1A). Vps15 flox/flox (Vps15$^{f/f}$) mice were viable and fertile and did not present any overt phenotype, indicating that the insertion of loxP does not alter *Vps15* gene function. Next, mice were crossed with transgenic mice overexpressing Cre under the human cytomegalovirus minimal promoter (CMV-Cre) (Schwenk et al, 1995) to excise DNA between the loxP sites in all tissues and generate whole body *Vps15*-deficient mice (Vps15$^{-/-}$) (Supporting Information Fig. 1A). Among 250 pups from the intercross of Vps15$^{f/-}$ mice, 168 had the Vps15$^{f/-}$ genotype, 82 were Vps15$^{f/f}$, but no Vps15$^{-/-}$ offspring was found, indicating that *Vps15*-mutant mice die during embryonic development. After timed matings, we did not witness *Vps15*-mutant embryos at as early as embryonic day (E) 7.5. Thus, we conclude that Vps15$^{-/-}$ embryos die during the implantation period before E7.5. The early embryonic lethality is similar to the phenotype of Vps34$^{-/-}$ mice (Zhou et al, 2011), while deletion of the *Atg5* and *Atg7* genes essential for autophagy
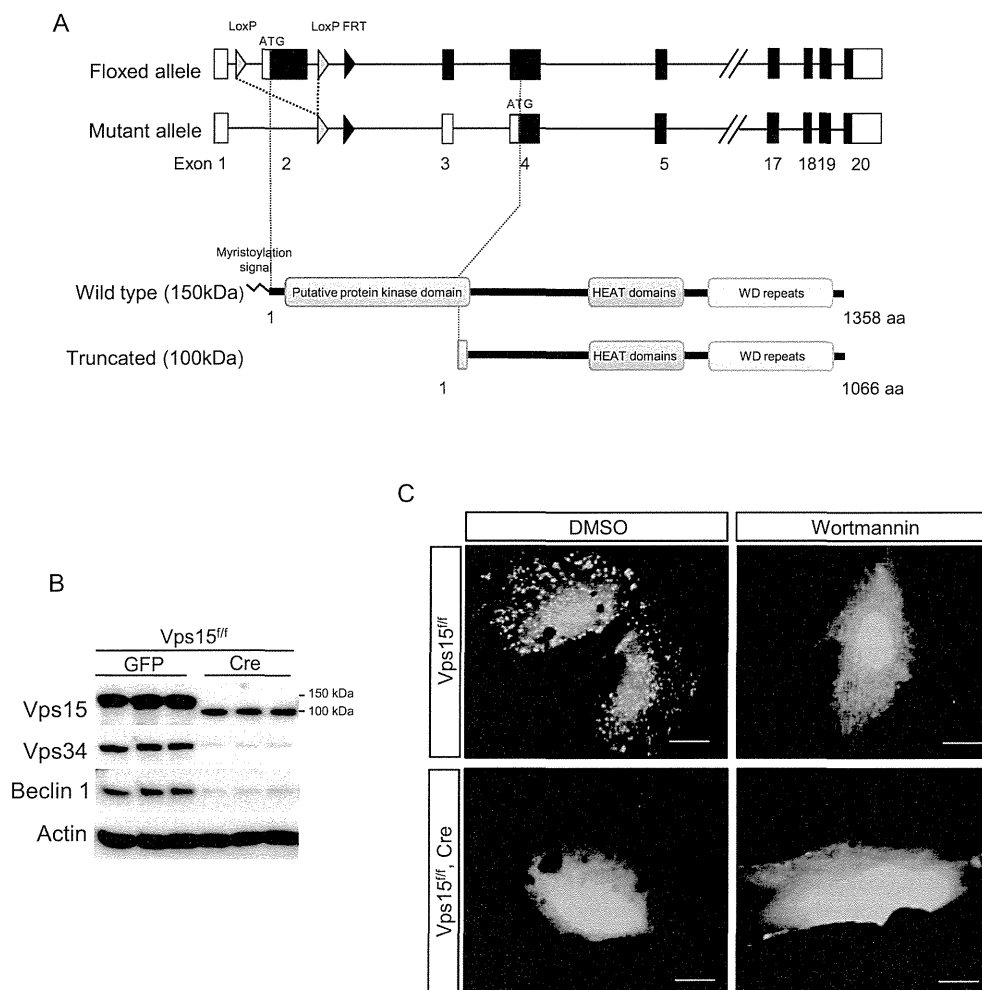
Figure 1. Generation and characterization of *Vps15*-null mice and cells.

A. Schematic representation of the targeted allele of *Vps15* gene and Vps15 protein domain structure. The coding exons are depicted by black boxes. The grey triangles denote *loxP* sequences, black triangle—FRT sequence. The putative protein kinase domain, HEAT domains (Huntingtin, elongation factor 3 (EF3), protein phosphatase 2A (PP2A) and the yeast kinase TOR1) and repeats of WD domain in the full-length and truncated Vps15 are depicted.

B. Immunoblot analysis of Vps15, Vps34 and Beclin 1 expression in MEF cells transduced with Adeno-Cre virus analysed 72 h post-infection.

C. *Vps15*-depleted MEFs were transfected with 2xFYVE-GFP expressing plasmid. 36 h post-transfection cells were treated with 200 nM wortmannin or DMSO alone for 30 min and PI3P positive compartments were visualised by confocal microscopy. Scale bars: 20 µm.

leads to perinatal lethality (Komatsu et al, 2005; Kuma et al, 2004). Taken together these data are consistent with Vps15 being required for Class III PI3K activity and having a broader role than autophagy regulation (Vanhaesebroeck et al, 2010).

To dissect signalling of *Vps15*-mutant cells, *Vps15* was deleted in cultures of Vps15[f/f] MEFs by adenoviral transduction of Cre recombinase. As shown in Fig. 1B, Cre expression resulted in the disappearance of full-length Vps15 protein. This was accompanied by the concomitant expression of a truncated Vps15 form of 100 kDa. We hypothesized that this short form arose from translation initiation at a start codon in exon 4 that is in frame with the one in exon 2. RTqPCR experiments confirmed

that this short Vps15 version lacked the N-terminus myristoylation signal and putative kinase domain (Supporting Information Fig. 1B). Importantly, the expression of the Vps15 partners, Vps34 and Beclin 1, was decreased after adenoviral Cre transduction (Fig. 1B), consistent with previous data indicating a role for Vps15 in stability of the complex (Thoresen et al, 2010), (Willinger and Flavell, 2012).

Since the best characterized biochemical function of Vps15/Vps34 complex is the production of PI3P (Vanhaesebroeck et al, 2010), we checked whether the PI3P production in *Vps15*-depleted cells was affected. For this purpose we used a reporter construct containing two FYVE domains fused with GFP (2xFYVE-GFP). As

– 30 –

FYVE domain binds PI3P in the cell, the fusion to GFP protein gives the opportunity to localize the endogenously produced PI3P (Stenmark and Aasland, 1999). As expected, transiently overexpressed 2xFYVE-GFP protein was localized in vesicular structures in Vps15$^{f/f}$ cells (Fig. 1C), consistent with the reported accumulation of PI3P in endosomes (Gaullier et al, 2000). Treatment with the PI3K inhibitor wortmannin resulted in a diffuse signal of 2xFYVE-GFP protein in Vps15$^{f/f}$ cells, providing a qualitative read-out of PI3P levels in the cell. Importantly, *Vps15* deletion mimicked the effect of wortmannin.

Induction of autophagosome formation is not impaired in *Vps15*-null MEFs

Autophagy is a major process controlled by the Vps15/Vps34 complex in yeast and mammalian cells (Simonsen and Tooze, 2009), though the level of regulation and the *in vivo* implications are unclear and require further work. Major PI3P-binding effectors that facilitate the formation of autophagosomes are the WD repeat domain phosphoinositide-interacting proteins 1 and 2 (WIPI-1 and 2), mammalian orthologues of yeast Atg18 (Codogno et al, 2011). Therefore, we transiently overexpressed mCherry tagged WIPI-1 protein in control Vps15$^{f/f}$ MEFs and after *Vps15* deletion by adenoviral Cre transduction. As expected, starvation in nutrient-deprived medium caused a sharp increase in mCherry-WIPI-1 positive puncta that was sensitive to wortmannin treatment in control cells (Fig. 2A). However, the number of cells presenting with mCherry-WIPI-1 positive puncta after starvation was dramatically lower in *Vps15*-depleted cells, although not completely abrogated. In addition, the size of the puncta was also reduced in mutant cells. These results were confirmed by immunostaining with antibodies directed against endogenous WIPI-2 (Fig. 2B). Taken together, our findings with FYVE-domain containing reporter proteins and endogenous PI3P effectors indicate that PI3P levels are sharply reduced upon *Vps15* depletion and that alternative mechanisms for PI3P production and WIPI regulation through other classes of PI3K or PIP phosphatases do not play a major compensatory role in *Vps15*-deficient MEFs.

Having demonstrated an impairment of PI3P signal transduction in *Vps15*-deficient cells, we asked the functional consequences on the autophagosome formation. The appearance of a faster migrating band of LC3 protein due to its lipidation and cleavage is a common marker of autophagy induction (Klionsky, 2007). As expected, in control Vps15$^{f/f}$ cells LC3 lipidation was blocked by wortmannin (Fig. 2C), consistent with a role of PI3K in autophagy initiation. However, in Cre-transduced cells, LC3 levels of both unlipidated and lipidated forms were increased as compared to GFP-transduced control, and lipidation was largely insensitive to wortmannin treatment. Strikingly, the increased levels of unlipidated and lipidated LC3 in Cre-transduced cells were also detected in basal nutrient-rich conditions (Fig. 2D). Next, we measured the levels of p62 protein, that functions as a cargo receptor for degradation of ubiquitinated proteins by the autophagosome (Rusten and Stenmark, 2010). Similar to LC3, p62 levels accumulated in *Vps15*-deficient cells even in basal conditions (Fig. 2D). To visualize autophagy, we performed microscopic analyses of *Vps15*-depleted and control cells to observe the presence of LC3 and p62 positive structures by EGFP-LC3 overexpression and immunostaining with anti-p62 antibody. In control cells in the presence of nutrients and growth factors the EGFP-LC3 staining was diffuse and p62 positive vesicles were scattered, indicating a low rate of autophagy (Fig. 2E). Strikingly, in *Vps15*-deficient cells numerous EGFP-LC3 and p62 positive structures were evident in nutrient-rich conditions. Counts of LC3 puncta showed a sixfold increase in mutant cells as compared to control (Fig. 2E). A significant fraction of p62 positive structures were also labelled by co-immunostaining with anti-Lamp2 or anti-Lamp1 antibodies, two common lysosomal markers (Fig. 2F and Supporting Information Fig. 2). Concomitantly, a sharp increase of ubiquitinated proteins and Lamp2 levels was detected in mutant cells using immunoblot analysis (Fig. 2G). In conclusion, LC3-positive autophagosomes are detected in *Vps15*-deficient cells, even in nutrient-rich conditions. Since LC3 and p62 are also substrates of the autophagy pathway, the massive amount of lysosomes containing p62 suggests impairment in terminal stages of autophagy after the fusion with lysosomes, leading to an accumulation of ubiquitinated proteins. Our findings suggest that the major functional defect after *Vps15* deletion in MEFs is subsequent to LC3 processing and autophagosome formation

Figure 2. Impaired autophagy in *Vps15*-depleted cells.

A. mCherry-WIPI-1 fails to form puncta in *Vps15*-depleted cells. MEFs were treated in nutrient free medium (EBSS) with or without 200 nM wortmannin, for 3 h and images were acquired by confocal microscopy. The number of mCherry-WIPI-1 puncta-positive cells in every treatment condition was determined from 200 individual cells ($n = 4$) by fluorescent microscopy (right panel). Scale bars: 20 μm. Data are mean ± SEM ($p \leq 0.01$ a: *vs.* control b: *vs.* Vps15$^{f/f}$) (left panel).

B. Endogenous WIPI-2 fails to form puncta in *Vps15*-depleted cells. MEFs were starved in nutrient free medium (EBSS) for 3 h and then fixed. WIPI-2 positive structures were visualized by immunofluorescence using anti-WIPI-2 antibody and images were acquired by confocal microscopy. Scale bars: 20 μm.

C. Immunoblot analysis of unprocessed and lipidated form of LC3 protein in *Vps15*-depleted cells. Cells were starved in HBSS medium with or without 200 nM wortmannin for 1 h. For protein analysis, the ratio of the densitometric assay of the two LC3 forms is presented. Data are mean ± SEM ($p \leq 0.05$ a: *vs.* CRE; b: *vs.* DMSO).

D. Immunoblot analysis of p62 and LC3 proteins in *Vps15*-depleted cells. To induce autophagy cells were starved in HBSS medium for 3 h. The ratio of the densitometric assay of the two LC3 forms is presented. Data are mean ± SEM ($p \leq 0.05$ a: *vs.* CRE; b: *vs.* 0 h).

E. p62-positive structures are co-localized with LC3 in *Vps15*-depleted MEFs. *Vps15*-depleted MEFs were infected with EGFP-LC3 expressing adenoviral vector and analysed by immunofluorescence using anti-p62 antibody. EGFP-LC3 puncta were counted in cells ($n = 40$ in Vps15$^{f/f}$, Cre and $n = 25$ in Vps15$^{f/f}$. Data are mean ± SEM ($p \leq 0.05$ a: *vs.* CRE).

F. Double-immunofluorescence staining of control and *Vps15*-depleted MEFs using anti-p62 and anti-LAMP2 antibodies. Scale bars: 10 μm.

G. Immunoblot analysis of total protein extracts of *Vps15*-depleted and control MEFs cells using anti-ubiquitin and anti-LAMP2 antibodies.
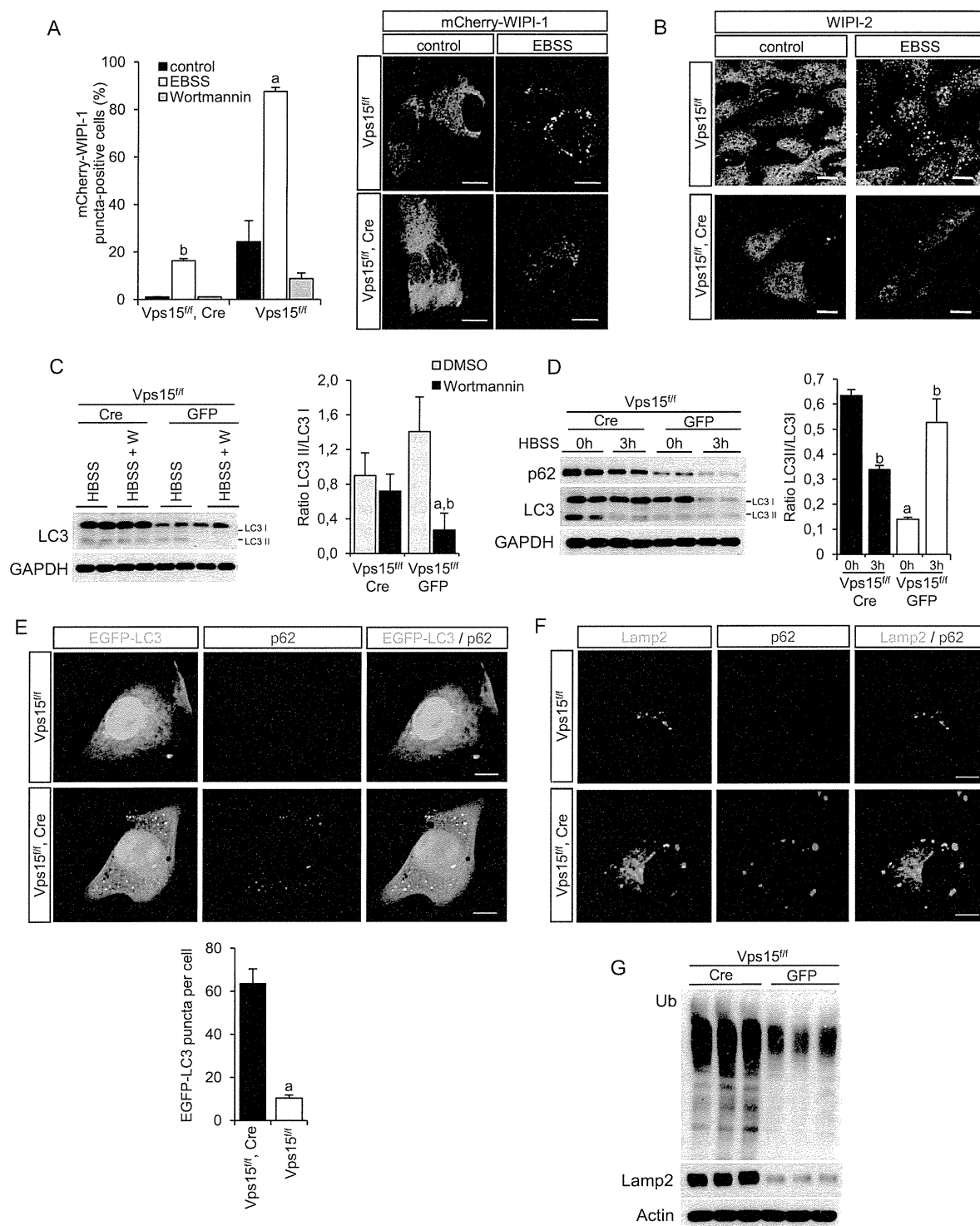
Figure 2.

that in mutant cells might be triggered by a wortmannin-insensitive pathway.

Autophagy flux is compromised in *Vps15*-depleted cells

To thoroughly follow autophagy flux from initiation to termination, we used monomeric Red Fluorescent Protein–Enhanced Green Fluorescent Protein (mRFP-EGFP) tandem fluorescent-tagged LC3 (tfLC3) (Kimura et al, 2007). tfLC3 emits both EGFP and mRFP signals before the autophagosome fusion with the lysosomes. However, the acidic lysosomal environment quenches the EGFP signal, while preserving the mRFP signal. In control MEFs after nutrient starvation, the numbers of both yellow (merged EGFP and mRFP signals) and red puncta were significantly increased, indicating active formation of both autophagosomes and autolysosomes (Kimura et al, 2007). Consistent with the analyses shown in Fig. 2, in *Vps15*-depleted cells the yellow puncta representing autophagosomes were predominant and detected both in basal and starved conditions (Fig. 3A). Importantly, the red puncta representing autolysosomes in mutant cells were lower as compared to control and were not induced by starvation. Next, we followed LC3 processing and p62 levels in presence of the lysosomal inhibitor bafilomycin A1, a known specific inhibitor of vacuolar-type H^+-ATPase (Fig. 3B and Supporting Information Fig. 3A). While in control cells this treatment led to the accumulation of processed LC3, in mutant cells the high levels of processed LC3 detected in basal conditions were not further increased by bafilomycin A1 treatment. In parallel, the p62 levels in mutant cells were also refractory to starvation and bafilomycin A1 treatment.

To further address lysosomal function in *Vps15*-depleted cells we employed betaine homo-cysteine methyltransferase (BHMT) assay (Mercer et al, 2008). In this assay the lysosomal activity is monitored by following the degradation of ectopically overexpressed GST-BHMT fusion protein. Previously, it has been established that GST-BHMT serves as a reporter of the autophagic flux as its delivery to the lysosome and degradation is dependent on macroautophagy pathway (Dennis and Mercer, 2009). As presented in Fig. 3C, upon autophagy induction condition the fragmentation of GST-BHMT reporter is severely impaired in *Vps15*-depleted MEFs compared to control cells. Taken together, our data are consistent with compromised Vps15/Vps34 signalling causing a block in autophagy flux after LC3 processing and autophagosome formation, and before lysosomal clearance. To address the possible cause of the low

lysosomal activity in *Vps15*-depleted cells we assayed the activities of several lysosomal enzymes. As presented in Fig. 3D, the activities of the tested lysosomal enzymes were significantly decreased in the extracts of *Vps15*-depleted cells as compared to control cells. Concurrently, we detected a significant increase in the activities of the same enzymes with the exception of α-mannosidase in the cell culture media. These results indicate that lysosomal enzymes are mistargeted in *Vps15*-depleted cells during the endosomal transport from the trans Golgi network and are excreted to the culture medium, contributing to the low lysosomal activity observed in mutant cells.

Nutrient signalling to mTOR is not significantly affected in *Vps15*-null MEFs

Whether the Vps15/Vps34 complex directly regulates amino-acid sensing and mTOR complex 1 (mTORC1) activation, is still an open question with conflicting reports (Juhasz et al, 2008; Nobukuni et al, 2005; Yoon et al, 2011; Zhou et al, 2011). In addition, the alteration of lysosomal mass and p62 levels that we observe in $Vps15^{-/-}$ cells, could also indirectly impact on mTORC1 activation by amino-acids, as lysosomes and p62 play an important role in this regulatory mechanism (Duran et al, 2011; Zoncu et al, 2011). To address the status of mTOR signalling in *Vps15*-depleted cells, we treated nutrient starved cells with growth factors in dialysed serum or with amino acid mixture, and assessed mTORC1 activity by immunoblot analysis with antibodies against phospho-Thr389 S6K1 or phospho-Ser240/244 rpS6. As shown in Fig. 4A, *Vps15* depletion led to a minor decrease and slower kinetics of mTORC1 activation by growth factors. Upon amino acid stimulation phosphorylation of mTORC1 targets was not dramatically changed even if we observed a tendency of mTORC1 activity to be increased over prolonged time period in cells lacking Vps15 (Fig. 4B). Our data do not support a positive requirement for Vps15/Vps34 in amino acid-stimulated mTOR activity. The minor activation of mTORC1 signalling by amino acids observed in *Vps15*-deficient cells may be consistent with the adaptive augmentation in lysosome mass and p62 levels observed in these cells (Fig. 2F). Interestingly, the PI3K inhibitor wortmannin decreased amino acid stimulated mTOR-signalling in both wild type and *Vps15*-deficient cells with similar potency (Fig. 4C), suggesting that additional PI3K classes distinct from Class III participate in this regulation.

To rule out the potential contribution in observed phenotype of the truncated Vps15 form that was generated by our gene

Figure 3. Autophagy flux is diminished in *Vps15*-depleted MEFs. ▶

A. *Vps15*-depleted and control MEFs were transduced with tfLC3 adenovirus. 48 h post-infection cells were either kept in full medium or starved in EBSS medium for 2 h, fixed and analysed by microscopy. Insets show higher magnification views. Counts of average number of yellow and red puncta per cell is presented on the graphs. Data are mean ± SEM ($n = 40$, $p \leq 0.05$, a: *vs.* Vps15$^{f/f}$ cells, b: *vs.* untreated). Scale bars: 10 μm.

B. Immunoblot analysis of total protein extracts of *Vps15*-depleted MEFs treated with EBSS for 2 h with or without 200 nM bafilomycin A1 using indicated antibodies. The ratio of p62 to actin and ratio of two LC3 forms of the densitometric assay is presented.

C. Immunoblot analysis of the Glutation sepharose eluates using anti-GST antibody. *Vps15*-depleted or control MEFs were transfected with plasmid expressing GST-BHMT, 24 h post-transfection cells were treated with EBSS supplemented with non-essential amino acids, E64d (6 μM) and leupeptin (11 μM) for 6 h to induce accumulation of lysosome-derived GST-BHMT proteolytic fragment. Total proteins were extracted and GST-fusion fragments precipitated using Glutation sepharose.

D. Lysosomal enzymes activity in the extracts of control and *Vps15*-depleted MEFs and in culture media. Equal numbers of *Vps15*-depleted or control cells were plated. The media was changed to fresh 24 h before collecting. The cell pellets and culture media were collected at day 6 post-infection. Data are mean ± SEM ($n = 6$, $p \leq 0.05$ a: *vs.* Vps15$^{f/f}$).
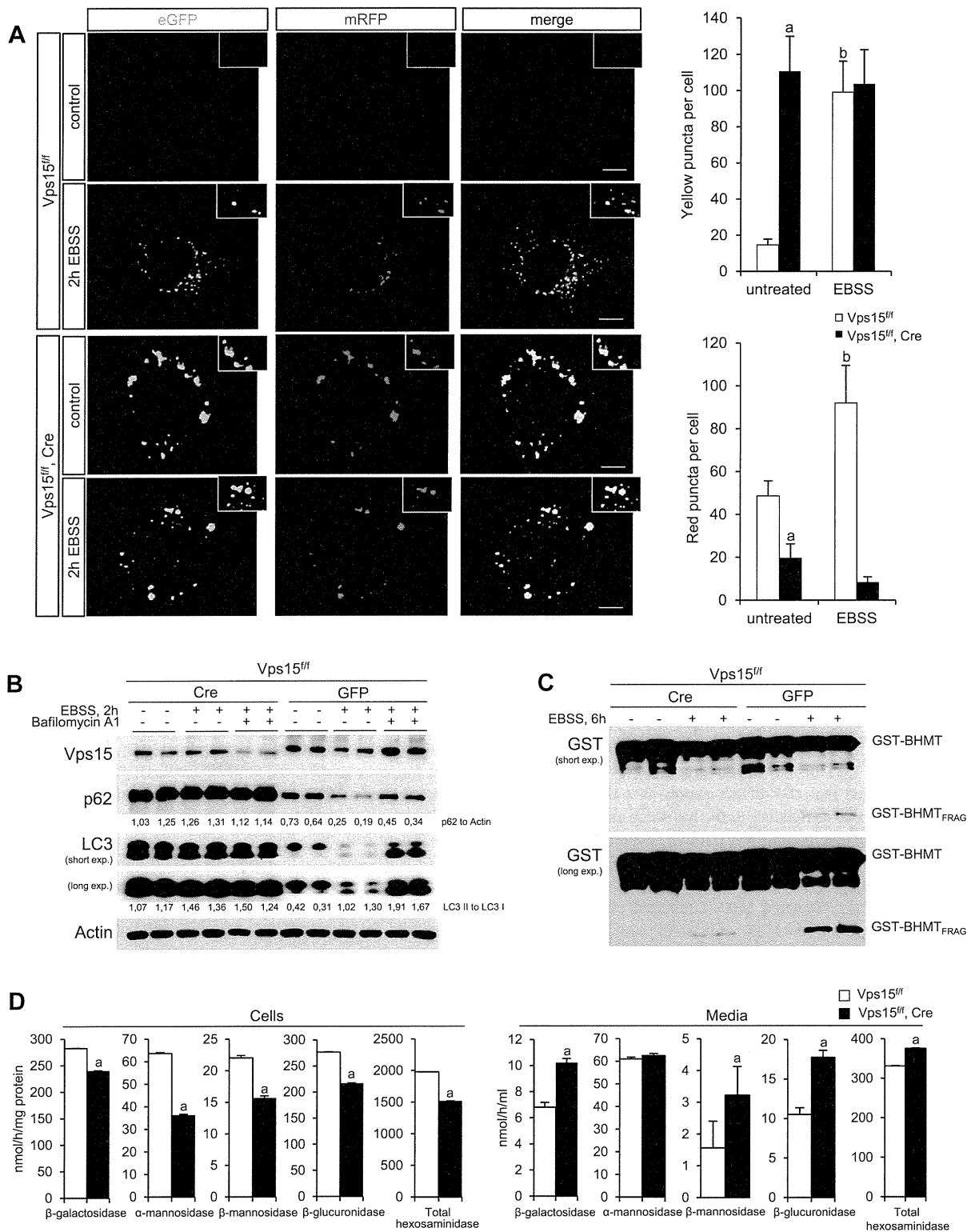
– 33 –

A

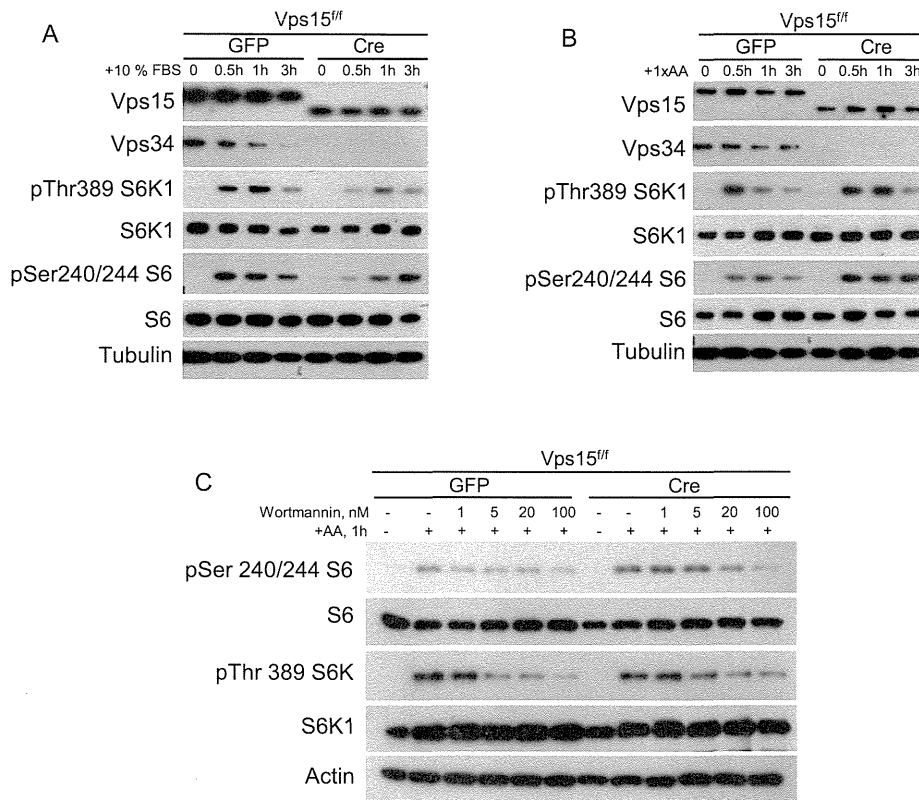
B

C

D

Figure 3.

Figure 4. Growth factor and nutrient signalling in Vps15-depleted MEFs.

A,B. Growth factor and nutrient stimulated signalling in Vps15-depleted cells. GFP or CRE adenovirus transduced MEFs were nutrient starved and then stimulated with dialysed FBS or cocktail of amino acids for indicated times. Total protein extracts were immunobloted with indicated antibodies.

C. Dose-dependent inhibition of mTOR activation by wortmannin. Immunoblot analysis with indicated antibodies of GFP or CRE adenovirus transduced MEFs which were nutrient starved and then treated with indicated doses of wortmannin or DMSO for 1 h before stimulation with a cocktail of amino acids for additional 1 h.

targeting strategy, we overexpressed the 100 kDa Vps15 protein by adenoviral transduction in wild type cells. As shown in the Supporting Information Fig. 3B, the truncated Vps15 did not affect the lysosomal mass as measured by Lamp2 immunoblot, the p62 and LC3 levels, the LC3 lipidation as well as the mTORC1 signalling. Furthermore, unlike full-length endogenous Vps15, the truncated 100 kDa Vps15 protein could not be immunoprecipitated in the complex with Beclin 1 or Vps34 (Supporting Information Fig. 3C). Thus the truncated Vps15 cannot form protein complexes with Class III PI3K activity and does not acquire signalling properties that could explain the effects of the gene targeting strategy on lysosomal function and mTOR signalling.

Deletion of Vps15 in skeletal muscles results in severe muscle damage

To address the physiological function of Vps15 *in vivo* and to overcome the embryonic lethality of Vps15$^{-/-}$ mice, we generated skeletal muscle specific knockout of Vps15 (muscle Vps15 KO), by crossing Vps15$^{f/f}$ mice with a transgenic line expressing Cre recombinase under the control of Human

Skeletal Actin promoter (Miniou et al, 1999). The presence of deleted allele was confirmed by PCR analysis of genomic DNA purified from skeletal muscle (Supporting Information Fig. 4A). Muscle Vps15 KO mice were born at the expected Mendelian ratio and had similar growth curves as compared to Cre-negative littermates (Supporting Information Fig. 4B). In addition, muscle Vps15 KO mice did not present an overt deterioration in nutrient homeostasis, as indicated by the normal glucose tolerance test (GTT) and insulin tolerance test (ITT) (Supporting Information Fig. 4C and D). Depletion of Vps15 was confirmed by immunoblot analyses of tibialis anterior (TA) muscle from 2 month old animals where Vps15 protein levels were significantly reduced (Fig. 5A). The residual detection of full length Vps15 protein in the muscle extracts from mutant mice may be due to incomplete excision, though the contribution of cell types other than differentiated muscle fibres within the tissue could not be excluded. Depletion of Vps15 in skeletal muscles resulted in decreased levels of Vps34 and Beclin 1 partners in the complex, and accumulation of p62 and LC3. Consistent with the observations in amino acid-stimulated MEFs, a minor activation of mTORC1 signalling to S6K1 and 4E